Published in: Cancer Research (2008), vol. 68, iss. 22, pp. 9541-950
Status: Postprint (Author's version)

ADAMTS-1 Metalloproteinase Promotes Tumor Development through the Induction of a Stromal Reaction *In vivo*

Natacha Rocks, Geneviève Paulissen, Florence Quesada-Calvo, Carine Munaut, Maria-Luz Alvarez Gonzalez, Maud Gueders, Jonathan Hacha, Christine Gilles, Jean-Michel Foidart, Agnès Noel[1], and Didier D. Cataldo[1]

Laboratory of Biology of Tumors and Development, Groupe Interdisciplinaire de Génoprotéomique Appliquée (GIGA)-Research, GIGA-Cancer and GIGA-I[3], University of Liege and CHU of Liège, Liège, Belgium

Abstract

ADAMTS-1 (a disintegrin and metalloproteinase with thrombospondin motifs), the first described member of the ADAMTS family, is differentially expressed in various tumors. However, its exact role in tumor development and progression is still unclear. The aim of this study was to investigate the effects of ADAMTS-1 transfection in a bronchial epithelial tumor cell line (BZR) and its potential to modulate tumor development. ADAMTS-1 overexpression did not affect *in vitro* cell properties such as (*a*) proliferation in two-dimensional culture, (*b*) proliferation in three-dimensional culture, (*c*) anchorage-independent growth in soft agar, (*d*) cell migration and invasion in modified Boyden chamber assay, (*e*) angiogenesis in the aortic ring assay, and (*f*) cell apoptosis. In contrast, ADAMTS-1 stable transfection in BZR cells accelerated the *in vivo* tumor growth after s.c. injection into severe combined immunodeficient mice. It also promoted a stromal reaction characterized by myofibroblast infiltration and excessive matrix deposition. These features are, however, not observed in tumors derived from cells overexpressing a catalytically inactive mutant of ADAMTS-1. Conditioned media from ADAMTS-1-overexpressing cells display a potent chemotactic activity toward fibroblasts. ADAMTS-1 overexpression in tumors was associated with increased production of matrix metalloproteinase-13, fibronectin, transforming growth factor β (TGF-β), and interleukin-1β (IL-1β). Neutralizing antibodies against TGF-β and IL-1β blocked the chemotactic effect of medium conditioned by ADAMTS-1-expressing cells on fibroblasts, showing the contribution of these factors in ADAMTS-1-induced stromal reaction. In conclusion, we propose a new paradigm for catalytically active ADAMTS-1 contribution to tumor development, which consists of the recruitment of fibroblasts involved in tumor growth and tumor-associated stroma remodeling.

INTRODUCTION

The evolution of a carcinoma depends not only on the acquisition of new properties by neoplastic cells but also on complex interactions occurring between the latter and the micro-environment (1). It is becoming increasingly clear that tumor stroma undergoes significant remodeling leading to the elaboration of a permissive environment for the vascularization, growth, and invasion of tumor cells (2-4). Fibroblasts are predominant cells in carcinoma-associated stroma and contribute to cancer progression through their production of growth factors and/or matrix degrading proteinases such as metalloproteinases (2, 5-7). The up-regulation of matrix metalloproteinases (MMP) is one of the physiologic changes that occur when fibroblasts undergo senescence and likely contributes to the higher frequency of cancers associated to aging (8).

The ADAMTS (a disintegrin and metalloproteinase with thrombospondin motifs) are MMP-related enzymes (9, 10). Their multidomain structure endows these secreted proteins with various functions. Some ADAMTS participate in different steps of cancer progression including cell proliferation, apoptosis, migration, invasion, and angiogenesis (11,12). Over the last few years, the list of substrates for ADAMTS has increased and includes type I and type II procollagens amino-propeptides, heparin-binding epidermal growth factor-like growth factor (HB-EGF), integrins, and E-cadherins (13-16).

Altered levels of ADAMTS have been documented in various cancers (12, 17-20). For instance, ADAMTS-1 production is modulated in lung, breast, or pancreatic cancers (18, 20, 21). The potential role of ADAMTS-1 in cancer progression is, however, not yet clearly defined because experimental studies in mice led to controversial data (22-24). A partial explanation for these discrepancies has been provided by the elegant study of Liu and colleagues (24) revealing that although the full-length ADAMTS-1 promotes metastasis, its -NH_2 or -COOH fragments lacking the catalytic activity display an inhibitory effect against metastasis.

[1] A. Noel and D.D. Cataldo should be considered as co-senior authors

The aim of the present work was to explore the contribution of ADAMTS-1 in lung cancer progression through the generation of ADAMTS-1-overexpressing human BZR cancer cells and to investigate the effect of ADAMTS-1 on the elaboration of a permissive microenvironment *in vivo*. For the first time, we provide evidence that catalytically active ADAMTS-1 induces a stromal reaction *in vivo* through the recruitment of fibroblastic cells and promotes tumor growth. This study provides new insight on the implication of an ADAMTS proteinase in the interplay between tumor cells and stromal cells.

MATERIALS AND METHODS

Cell culture

Human lung carcinoma BZR cells and human lung fibroblasts were obtained from American Type Culture Collection. Cells were grown at 37°C in 5% CO_2 in DMEM supplemented with 10% fetal bovine serum, 2 mmol/L L-glutamine, and penicillin-streptomycin (100 IU/mL-100 μg/mL). Culture reagents were purchased from Invitrogen Corp./Life Technologies.

Preparation of cDNA constructions, mutagenesis, and transfection of BZR cells with human *ADAMTS-1* or *ADAMTS-1 E/Q* cDNA.

Full-length wild-type human *ADAMTS-1* cDNA (hADAMTS-1; OriGene) was subcloned at *Not*I sites into pcDNA3.1-*zeo* mammalian expression vector (Invitrogen) under the control of the cytomegalovirus promoter. An amino acid-substituted mutant of *ADAMTS-1, E386Q,* was constructed by mutagenesis based on a PCR technique (Stratagene). The nucleotide sequences of the mutants were confirmed by direct sequencing. The recombinant plasmids or the empty pcDNA3.1-*zeo* vector used as control was stably transfected into BZR cells by electroporation in serum-free medium at 250 V and 960 μF using a gene puiser system (Bio-Rad Laboratories). Transfected populations were subjected to a selective pressure of zeocin (6 mg/mL; Invitrogen). Clones were screened by semiquantitative reverse transcription-PCR (RT-PCR) and Western blotting for ADAMTS-1 expression.

Preparation of conditioned media, mRNA and protein cell/tissue extracts.

Cells (10^6) were seeded in 100-mm-diameter Petri dishes (Falcon, Becton Dickinson) in serum-containing medium for 24 h. After 48 h of culture in serum-free medium, conditioned media were harvested, clarified by centrifugation, and stored at -20°C. Total protein cell extracts were prepared from cell monolayer by incubation for 15 min in radioimmune precipitation assay buffer [50 mmol/L Tris-HCl (pH 7.4), 150 mmol/L NaCl, 1% NP40, 1% Triton X-100, 1% sodium deoxycholate, 0.1% SDS, 5 mmol/L iodoacetamide, 2 mmol/L phenylmethylsulfonyl fluoride]. After a 20-min centrifugation (10,000 rpm), supernatants were stored at -20°C. Total proteins were extracted from tumor tissues by incubating the crushed tissue with a lysis buffer (40 mmol/L Tris, 20% sucrose) containing 2% SDS. Protein concentrations were determined using DC protein Assay kit (Bio-Rad Laboratories). Total RNA was extracted from cell monolayer or tumor tissues using High Pure RNA Isolation kit or High Pure RNA Tissue kit, respectively (Roche Diagnostic Applied Science), as recommended by the manufacturer.

Semiquantitative RT-PCR analysis.

RT-PCR was done on 10 ng of total RNA using the GeneAmp thermostable *rTth* RT-PCR kit (Applied Biosystems). Primers (Eurogentec) used in this study were designed as follows: *ADAMTS-1,* 5'-CAGCCCAAGGTTGTAGATGGTA-3' (sense) and 5'-GAGCCACCAACATCGAAGTGAA-3' (antisense); interleukin-1β (*IL-1β*), 5'-AAACAGATGAAGTGCTCCTTCAGG-3' (sense) and 5'-TGGAGAACACCACTTGTTGCTCCA-3' (antisense); *MMP-1,* 5'-GAGCAAACACATCTGAGG-TACAGGA-3' (sense) and 5'-TTGTCCCGATGATCTCCCCTGACA-3' (antisense); *MMP-8,* 5'-CCAAGTGGGAACGCACTAACTTGA-3' (sense) and 5'-TGGAGAATTGTCACCGTGATCTCTT-3' (antisense); *MMP-13,* 5'-ATGA-TCTTTAAAGACAGATTCTTCTGG-3' (sense) and 5'-TGGGATAACCTTCCA-GAATGTCATAA-3' (antisense); *MMP-14,* 5'-GGATACCCAATGCC-CATTGGCCA-3' (sense) and 5'-CCATTGGGCATCCAGAAGAGAGC-3' (antisense); transforming growth factor-β (*TGF-β*), 5'-GGAGAGGGCCCAG-CATCTGCAA-3' (sense) and 5'-TGTACTGCGTGTCCAGGCTCCAA-3' (antisense); and *28S,* 5'-GTTCACCCACTAATAGGGAACGTGA-3' (sense) and 5'-GATTCTGACTTAGAGGCGTTCAGT-3' (antisense). RT-PCR products were resolved on 10% polyacrylamide gels and quantified by Fluor-S Multimager (Bio-Rad Laboratories) after Gelstar staining (Sanvertech). To normalize mRNA levels in different samples, results are expressed as a ratio between the

intensity of each band and that of the corresponding 28S rRNA value.

Western blotting and ELISA

Samples (conditioned medium, cell or tissue lysates; 20 μg of total protein extracts) were separated under reducing conditions on polyacrylamide gels and transferred on polyvinylidene difluoride membrane (NEN). After blocking in PBS containing 10% nonfat milk and Tween 20 (0.05%), membranes were incubated overnight at 4°C with the primary antibody rabbit polyclonal anti-ADAMTS-1 (Sigma Aldrich), mouse polyclonal anti-MMP-13 (Fuji Chemical Industries), rabbit polyclonal anti-collagen I, mouse monoclonal anti-TGF-β (Abcam), or mouse polyclonal anti-fibronectin (Sigma Aldrich). Immunoreactive proteins were visualized using the corresponding secondary antibody conjugated with horseradish peroxidase (HRP; DAKO) and the enhanced chemiluminescence detection kit (Perkin-Elmer Life Sciences). As loading control, actin levels were determined. Results are expressed as ratio between measured protein levels and corresponding actin levels. IL-1β levels were assessed using commercial ELISA (R&D Systems).

***In vitro* proliferation, migration, and invasion assays**

BZR cells were seeded in triplicates in 24-well plates on a plastic substrate (two-dimensional culture) or embedded in a type I collagen gel (2 mg/mL; three-dimensional culture) and maintained in standard culture conditions for up to 12 or 7 d, respectively. Cells were harvested at various time intervals. Cells were extracted from collagen gels by a 1-h treatment with bacterial collagenase (1 mg/mL; Sigma Aldrich) at 37°C. The DNA content of sonicated cell suspensions was determined by fluorimetry using *bis*-benzimidazol H33258 reagent (Hoechst; ref. 25). Anchorage-independent growth was determined by soft agar assay (26). Cells were plated into 24-well plates in growth medium containing 0.3% agar, on top of a 0.6% agar gel. After 9 d, cells were stained with crystal violet for 1 h and photographed. Colonies were counted under a microscope at x2 magnification. Each assay was done in triplicate in two independent assays.

For chemotaxis or chemoinvasion assays, uncoated or Matrigel-coated (25 μg/filter) filters (8-μm pore, Nucleopore) were used in 48-well invasion chamber (Neuroprobe), respectively. Lower wells were filled with 30 μL DMEM supplemented with 10% fetal bovine serum and 1% bovine serum albumin (BSA), media conditioned by *ADAMTS-1* -transfected cells, or media conditioned by control populations. In some assays, recombinant ADAMTS-1 (5 μg/mL; R&D Systems), anti-TGF-β (0.1 μg/mL; Abcam), and/ or anti-IL-1β (1 ng/mL; R&D Systems) neutralizing antibodies were added in the lower wells. Cells were suspended in serum-free medium supplemented with 0.1% BSA (Fraction V, Acros Organics) and placed in the upper wells. Chambers were incubated at 37°C for 4 h (for fibroblast migration) or 6 h (for BZR migration and invasion). Cells having reached the lower surface of the filter were counted under a microscope at x400 magnification (30 random fields). Results are expressed as mean number of migrating or invading cells per 30 fields ± SE and are those of one representative experiment done at least twice (each experimental condition done in quadruplicates).

Apoptosis measured by terminal deoxyribonucleotidyl transferase-mediated dUTP nick end labeling assay

BZR transfectants were seeded at 5×10^3 cells per well in triplicates onto 24-well plates. After adhesion, cells were stimulated or not with etoposide (20 μmol/L; Calbiochem) for 24 h. Cells were then harvested for terminal deoxyribonucleotidyl transferase-mediated dUTP nick end labeling (TUNEL) staining. The proportion of cells showing DNA fragmentation was measured by incorporation of FITC-12-dUTP into DNA using terminal deoxynucleotidyl-transferase (In Situ Cell Death Detection, Roche Diagnostic Applied Science) as described by the manufacturer. To determine total cell number, cell nuclei were labeled with bis-benzimide. The total number of cells and the number of TUNEL-labeled cells were counted in six random fields at x400 magnification. Quantitative analysis of apoptosis is represented as the mean of the ratio of TUNEL-labeled cells by total number of cells (%) ± SE. Experiments were done at least twice in triplicates.

***In vitro* angiogenesis assessment: the aortic ring assay**

Rat aortic expiant cultures were prepared as previously described (27). Briefly, 1-mm-long aortic rings were embedded in three-dimensional collagen gels and cultured in MCDB131 medium (Invitrogen) supplemented with media conditioned by ADAMTS-1 or control clones (volume/volume; ref. 28). Vascular endothelial growth factor (VEGF; 20 ng/mL) was used as a positive control. The cultures were kept at 37°C and examined every second day with a Zeiss microscope. Images were captured on days 6 and 9 for computerized quantification of the number of vessels formed according to previously described methods (28).

Assessment of tumor development *in vivo*

Male severe combined immunodeficient (SCID) mice (Harlan), 6 to 8 wk old, were used. Transfected BZR cell population or clone suspensions were prepared in serum-free DMEM and mixed with an equal volume of cold Matrigel (29). A final volume of 400 μL of mixed Matrigel and serum-free medium containing 10^6 cells was injected into the flank of mice ($n = 15$). Tumor growth was assessed by measuring the length and width of tumors and the volume was determined by using the following formula (length) × $(\text{width})^2$ × 0.4 (ref. 29). Results from two independent assays are expressed as mean of tumor volumes of each experimental group ± SE. At the end of the experiment, animals were sacrificed and tumors and organs were resected. Half volumes of the tumor from experimental animals were fixed in 10% formalin and embedded in paraffin for histologic analysis. The other half of tumor was frozen in liquid nitrogen until use. Experiments were approved by the animal ethical committee of the University of Liege.

Immunohistochemistry

Immunohistochemistry was done on 5-μm tumor sections. Sections were deparaffinized and, after unmasking antigens, treated with 3% H_2O_2 for 20 min to quench endogenous peroxidase activity. Blockade of nonspecific binding was done by incubation with PBS/BSA 10% (Fraction V, Acros Organics; for LYVE-1), normal goat serum [for smooth muscle actin (SMA) and von Willebrand Factor (vWF)], or normal rabbit serum [for proliferating cell nuclear antigen (PCNA)] for 30 min. Sections were then incubated for 1 h with a mouse monoclonal anti-PCNA (DAKO; 1:400), a mouse monoclonal anti-SMA (DAKO; 1:200), a rabbit polyclonal anti-vWF (DAKO; 1:200), or a rabbit polyclonal anti-LYVE-1 (kindly provided by K Alitalo, University of Helsinki, Helsinki, Finland; 1:1,200). After several washes, slides were incubated with rabbit anti-mouse HRP-coupled secondary antibody (DAKO; 1:100; for PCNA) or with a biotin-coupled secondary antibody (DAKO; 1:400) followed by incubation with streptavidin/HRP complex (DAKO; 1:500; for SMA vWF, and LYVE-1). Peroxidase activity was revealed with the 3,3'-diaminobenzidine hydrochloride kit (DAB, DAKO). Slides were counterstained with hematoxylin, mounted, and observed under a microscope.

For H&E-saffron staining, sections were deparaffinized and first stained with Mayer's hematoxylin (Biogenex). After several washes, slides were dehydrated in ethanol and stained for 30 min with alcoholic safranin O (safranin 0.6% in 20% ethyl alcohol; Sigma Aldrich), rinsed, and mounted.

The yellow saffron staining and immunostainings were measured using Image J program. Results are expressed as the ratio between the surface of immunostaining and the total surface of tumor tissue analyzed. A minimum of 140 representative sections of each group were used for quantification.

In situ hybridization for Y mouse chromosome

Hybridization was done on serial paraffin sections. Slides were deparaffinized and dehydrated in ethanol 100%. After incubation in HCl 2N for 20 min, slides were rinsed thrice in 2x SSC (Promega) and incubated at 80°C for 15 min in sodium sulfocyanate (Sigma Aldrich) for cytoplasm denaturation. Slides were washed in 2x SSC and nucleus proteins were denatured for 5 min with proteinase K (Roche Diagnostic Applied Science). After incubation in PBS/$MgCl_2$/4% formaldehyde, sections were dehydrated in ethanol and dried for hybridization. Slides were then denatured for 5 min at 72°C on a heating block and hybridized with a mouse FITC chromosome Y labeled probe (Cambio) for 18 h in a humidified chamber at 37°C. Washes at 72°C in 1 x SSC/0.3% Tween 20 and then in 2x SSC were done before dehydration. After HRP staining with an anti-FITC-HRP antibody (Roche Diagnostic Applied Science), slides were counterstained with hematoxylin, mounted, and observed under a microscope.

Hydroxyproline quantification of tumor tissue

Tumor tissues were hydrolyzed for 3 h at 137°C in 6 mol/L HCl. Hydroxyproline content was determined with a color-based reaction as described by Bergmann and Loxley (30). The standard curve used for hydroxyproline ranged from 0 to 3 mg/mL. For normalization, hydroxyproline values were divided by the dry mass of tissue hydrolyzed.

Statistical analysis

Statistical differences were assessed between the *in vivo* experimental groups using Mann-Whitney test (*, $P < 0.05$; **, $P < 0.01$; ***, $P < 0.001$).

Published in: Cancer Research (2008), vol. 68, iss. 22, pp. 9541-950
Status: Postprint (Author's version)

Figure 1: *Characterization of stable BZR ADAMTS-1 transfectants and in vitro cell proliferation.* *A*, RT-PCR (*mRNA*) and Western blot analysis (protein) of ADAMTS-1-expressing clones (*AD1-AD3*), ADAMTS-1-overexpressing population (*ADp*), control clones (*C1-C3*), and control population (*Cp*). Protein production was analyzed in cell lysates (cell) and in medium conditioned by cells (medium) as described in Materials and Methods. Expression of 28S rRNA (*A*) and production of actin (β) were used to ascertain equal loading. *L*, molecular marker. *B* to *D*, *ADAMTS-1*-transfected clones (*AD1-AD2*), control clones (*C1-C2*), and their corresponding populations (*ADp and Cp*) were cultured for various periods of time on plastic (*B*), in a collagen gel (*C*), or in a soft agar gel (*D*). Cell proliferation was measured by determining the DNA content (*B and C*) or by counting cell colonies after crystal violet staining (*D*) as described in Materials and Methods.

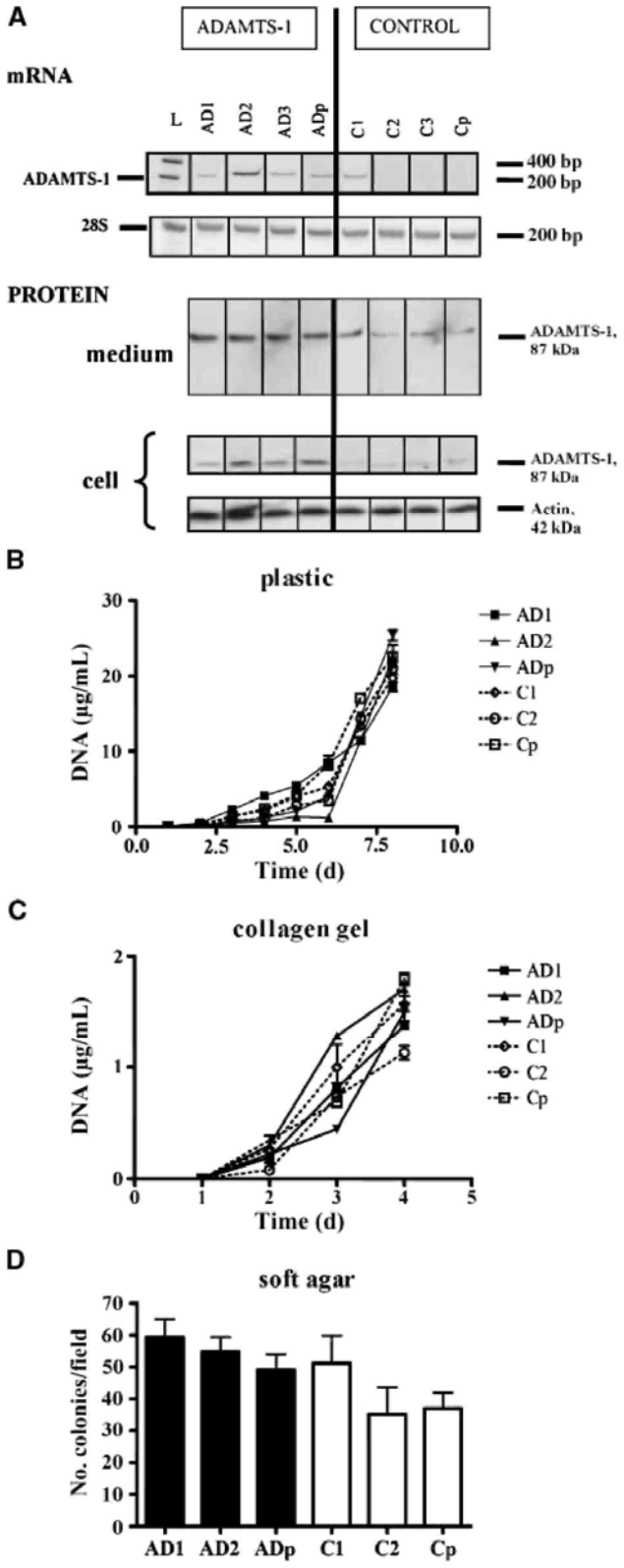

Published in: Cancer Research (2008), vol. 68, iss. 22, pp. 9541-950
Status: Postprint (Author's version)

RESULTS

Generation and *in vitro* characterization of BZR ADAMTS-1 stable transfectants

Human BZR cells were stably transfected with pcDNA3.1-*zeo* vector containing the full-length *ADAMTS-1* cDNA (Fig. 1*A*) or with the empty pcDNA3.1-*zeo* plasmid as a control. Cell populations and clones obtained by zeocin selection were screened for ADAMTS-1 mRNA expression by RT-PCR and protein production by Western blotting (Fig. 1*A*). Three ADAMTS-1-overexpressing clones (AD1-AD3) and three control clones (C1-C3), as well as the corresponding populations (ADp or Cp), were selected for further *in vitro* and *in vivo* studies. A protein band of 87 kDa corresponding to the expected size of the mature enzyme was detected by Western blot in cell lysates and in the medium conditioned by ADAMTS-1-expressing cells (Fig. 1A). No ADAMTS-1 fragment was visualized, indicating that the enzyme did not undergo any cleavage.

Clones and populations were then compared *in vitro* in their proliferative and invasive capacities. ADAMTS-1 expression did not affect the proliferation rate on a two-dimensional plastic support (Fig. 1B*)* or in a three-dimensional collagen gel (Fig. 1C). In addition, no statistical difference of anchorage-independent growth was observed in soft agar assay (Fig. 1D*)*. Moreover, the sensitivity of cells to etoposide was not affected by ADAMTS-1 overexpression, leading to similar apoptotic rates in all clones and populations, as assessed by the TUNEL assay (7.9 ± 2% for ADAMTS-1-overexpressing cells versus 5.8 ± 1.5% for control clones, $P = 0.55$). Transfected cells were tested for their ability to migrate through uncoated filters (migration assay) or to invade Matrigel-coated inserts (invasion assay) in modified 48-well Boyden chamber. The numbers of migrating or invading cells were found to be independent of ADAMTS-1 production (migration: 351 ± 53 for ADAMTS-1-overexpressing cells versus 364 ± 28 for control clones, $P = 0.66$; invasion: 541 ± 76 for ADAMTS-1-overexpressing cells versus 382 ± 37 for control clones, $P = 0.12$). Because ADAMTS-1 has been described as a modulator of angiogenesis, we investigated the ability of selected clones and populations to modulate *in vitro* angiogenesis. Therefore, rat aorta rings embedded in a collagen gel were cultured in MCDB culture medium supplemented with media conditioned by cells overexpressing ADAMTS-1 or control cells as previously described (29). Similar microvessel outgrowth was observed in all experimental conditions, suggesting that the secreted full-length ADAMTS-1 does not affect *in vitro* angiogenesis (number of vessels: 29 ± 4 for media conditioned by ADAMTS-1-overexpressing cells versus 37 ± 8 for media conditioned by control clones, $P = 0.35$).

Taken together, these data show that, *in vitro,* ADAMTS-1 did not modulate the tested cell properties (cell proliferation, anchorage-independent growth, apoptosis, chemotaxis, chemo-invasion, and angiogenesis induction).

ADAMTS-1-driven enhancement of tumor development *in vivo*

To further evaluate the *in vivo* tumorigenic phenotype of ADAMTS-1 transfectants and appropriate controls, clones and populations were s.c. injected into immunodeficient SCID mice. The volume of tumors derived from ADAMTS-1-overexpressing populations (ADp) was higher than that obtained with control populations (Cp; $P < 0.05$; Fig. *2A*). Similar results were obtained with individual clones (data not shown). Moreover, the progression of tumors derived from ADAMTS-1-expressing cells bearing a mutation in the catalytic domain (E/Q; ADp*) was similar to tumors derived from the corresponding control population (Fig. *2A).*

RT-PCR and Western blotting done on mRNA or proteins extracted from tumor samples (ADp and Cp) confirmed that higher ADAMTS-1 mRNA expression ($P < 0.01$) and protein production ($P < 0.05$) persisted *in vivo* in tumors induced by the injection of ADAMTS-1-overexpressing cells (Fig. *2B).* Cell proliferation rate was determined in tumor samples (ADp and Cp) by immunostaining against PCNA. The proliferation index was higher in ADAMTS-1-overexpressing tumors (ADp) as compared with controls (Cp; $P < 0.0001$; Fig. 2C).

ADAMTS-1 overexpression promotes a stromal reaction *in vivo*

Tumor vascularization was analyzed by immunostaining with vWF antibody, whereas LYVE-1 antibody was used to assess lymphangiogenesis. No obvious difference of blood or lymphatic vascularization was observed in tumors generated by the ADAMTS-1-overexpressing or control cells (data not shown). In sharp contrast, staining for α-SMA revealed the presence of increased number of α-SMA-positive cells in the stroma of tumors derived from ADAMTS-1 transfectants ($P < 0.001$). This observation implies a probable increased recruitment of host mesenchymal cells and their differentiation into myofibroblasts in ADAMTS-1-overexpressing tumors (Fig. 3A). The catalytic activity of ADAMTS-1 seems to play a key role in this process because tumors derived

from cells overexpressing an inactive mutant of ADAMTS-1 did not display an enhanced number of recruited host cells (Fig. *3A*). We then verified whether α-SMA-positive cells were issued from host tissues or from a possible transdifferentiation of tumor cells themselves. Because tumors have been xenografted in male recipient mice, *in situ* hybridization for Y mouse chromosome was applied and compared with α-SMA stainings on serial tumor sections. The α-SMA and mouse Y chromosome stainings were detected in host cells infiltrating the tumor and associated to connective tissue structures, rather than in tumor cells (Fig. 3B, *bottom).*

Figure 2: *ADAMTS-1 expression promotes in vivo tumor growth.* A, tumor volumes assessed after 31 d were determined and data are expressed as fold induction in tumors overexpressing ADAMTS-1 (*ADp*) or the mutated ADAMTS-1 (*ADp*)* relative to the corresponding control (Cp; $n = 38$ for ADAMTS-1-overexpressing populations and corresponding control populations; $n = 8$ for the mutated ADAMTS-1 populations and corresponding controls). Data are expressed as fold induction relative to tumor size obtained with corresponding control populations. *, $P < 0.05$. B, representative examples of ADAMTS-1 levels in tumor tissues measured by RT-PCR (*top*) and Western blotting (*bottom*). Higher ADAMTS-1 mRNA and protein levels were detected in tumors derived from ADAMTS-1 transfectants, as assessed by RT-PCR and Western blot, respectively ($n = 38$). C, PCNA immunostaining in tumors derived from ADAMTS-1-overexpressing cells (*ADp*) or control cells (*Cp*). Magnification, x400. *Right*, quantification of PCNA immunostaining (PCNA staining/total area). ***, $P < 0.001$.

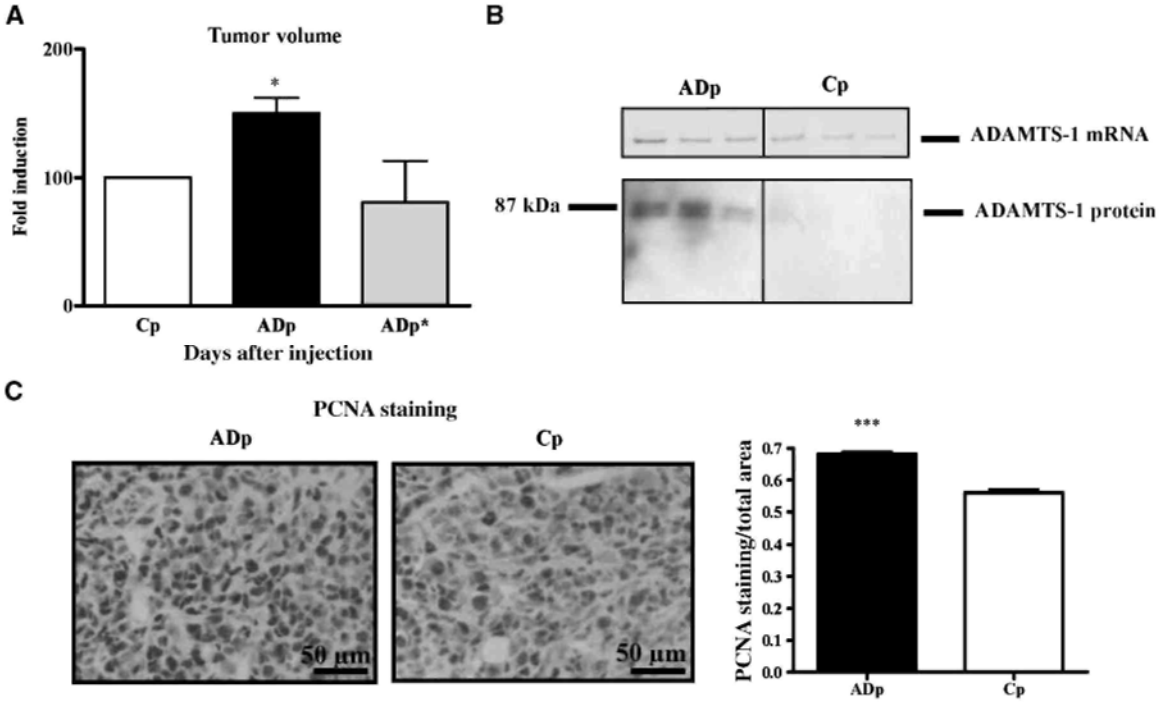

To get deeper insights into the stromal reaction observed in tumor tissues, saffron staining was done on tumor sections to label fibrillar collagens (Fig. 4*A*). The percentage of saffron-positive area was 1.9 times higher in tumors derived from ADAMTS-1-overexpressing cells as compared with tumors derived from control cells (17.6 ± 1.52% versus 9.2 ± 1.5%, $P < 0.01$; Fig. 4B). Collagen content in tumors derived from cells transfected with the proteinase-dead ADAMTS-1 did not show any differences when compared with collagen content observed in corresponding control tumors (6.47 ± 0.7% versus 4 ± 0.5%, $P > 0.05$).

Measurements of total hydroxyproline in extracts from tumors revealed that tumor collagen content was twice elevated in ADAMTS-1-overexpressing tumors as compared with controls ($P < 0.05$; Fig. 4*C*). This enhancement of collagen deposit was further confirmed by Western blot analysis revealing higher amounts of the different type I collagen chains in ADAMTS-1-overexpressing tumors (Fig. 4*D*). Fibronectin production was also increased in tumors overexpressing ADAMTS-1 ($P < 0.05$; Fig. 4*D*). Taken together, these results clearly point to an enhanced stromal reaction in ADAMTS-1-overexpressing tumors characterized by the recruitment of αSMA-positive cells and a higher collagen and fibronectin production.

Figure 3*: *ADAMTS-1 promotes the recruitment of host cells in tumors. A. α-SMA immunostaining done on tumor sections derived from ADAMTS-1 (*ADp*), control (*Cp*) populations, cells overexpressing a proteinase-dead ADAMTS-1 (*ADp**), and corresponding control population (*Cp2*; magnification, x200). Arrows delineate the presence of α-SMA-positive cells. Bottom, quantification of α-SMA immunostaining (α-SMA staining/total area). ***, $P < 0.001$. B. α-SMA immunostaining and in situ hybridization (*FISH*) for Y mouse chromosome. Top, positive control: murine vessel stained for α-SMA (*left*) and Y chromosome hybridization (*FISH; right*). Bottom, in situ hybridization for Y mouse chromosome and α-SMA stainings on serial sections are both localized on aligned cells in stromal structures (*arrows*; magnification, x400).

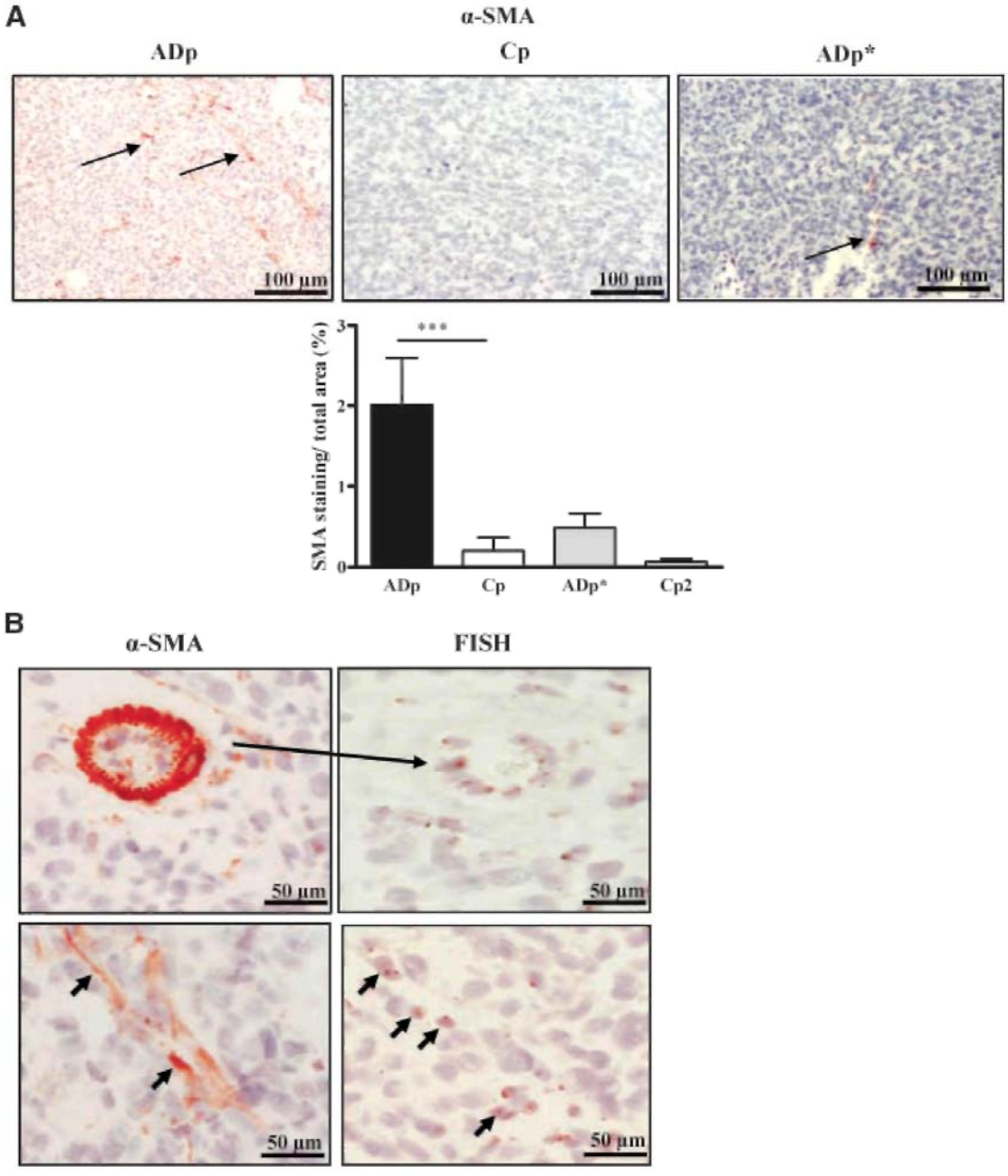

ADAMTS-1 overexpression affects the production of stromal reaction regulators

We next analyzed the modulation of putative mediators of fibroblast recruitment (IL-1β, TGF-β, platelet-derived growth factor, and placenta growth factor) and of collagen matrix remodeling (interstitial collagenases MMP-1, MMP-8, MMP-13, and MMP-14). Among these molecules tested by RT-PCR analysis, we found higher levels of IL-1β ($P < 0.05$), TGF-β ($P < 0.05$), and MMP-13 ($P < 0.01$) mRNAs in tissues derived from ADAMTS-1-overexpressing cells as compared with control tissues (Fig. *5A)*. In addition, mRNA levels of TGF-β ($P = 0.0009$; $r = 0.6028$) as well as MMP-13 ($P = 0.0004$; $r = 0.6402$) are correlated to the levels of ADAMTS-1

mRNA in tumor tissues. In all cases, protein analyses by Western blots or ELISA confirmed results obtained at the mRNA levels (Fig. *5B* and C). Such modulation of TGF- β and IL-1β by ADAMTS-1 was also found *in vitro*. Indeed, the amounts of TGF-β and IL-1β released by ADAMTS-1 transfectants cultured *in vitro* were higher than those produced by control cells (Fig. *5B* and *C*). However, it is interesting to note that only a faint nonmodulated MMP-13 expression was detected *in vitro* (data not shown). Altogether, these results show the effect of ADAMTS-1 overexpression on the modulation of mediators driving stromal reactions.

Figure 4: *ADAMTS-1 promotes the formation of stromal structures and the production of stromal matrix components.* A, saffron staining on primary tumors derived from ADAMTS-1 (*ADp*) or control cell populations (*Cp*) or cells overexpressing an inactivated ADAMTS-1 (*ADp**). Magnification, x400. B,quantification expressed as a percentage of the ratio between yellow saffron staining area and total tumor area analyzed. C, quantification of hydroxyproline in tumor extracts reflecting the collagen content. Hydroxyproline amounts were quantified on dried tumor tissues as described in Materials and Methods. D, representative example of Western blot analysis of α1 and α2 type 1 collagen chains (*left*) and fibronectin (*right*) in tumor extracts ($n = 30$). Bottom, quantifications done by densitometric scanning. **, $P < 0.01$; *, $P < 0.05$.

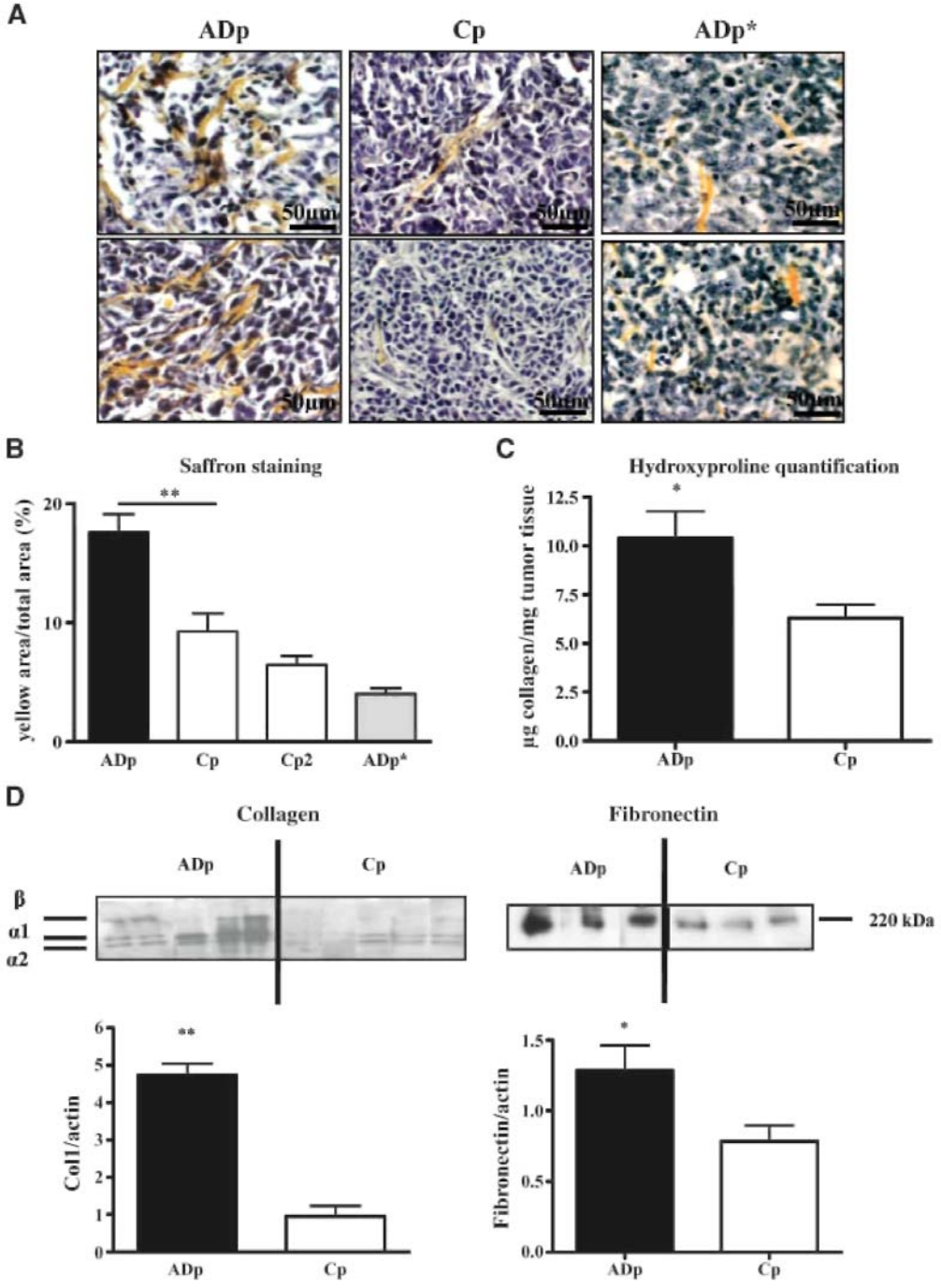

Published in: Cancer Research (2008), vol. 68, iss. 22, pp. 9541-950
Status: Postprint (Author's version)

Figure 5: *ADAMTS-1 affects the production of stromal reaction regulators.* RT-PCR (A), Western blot (B), or ELISA (C) analyses were done to measure MMP-13, TGF-β, or 1L-1β levels in tumor tissues ($n = 30$). 28S and actin are shown as loading controls. *Left,* representative examples of RT-PCR bands. The measurement of TGF-β and IL-1β levels has also been done *in vitro* in media conditioned by transfectants (*CM*). *B* and *D*, quantification was done by densitometric scanning. *, $P < 0.05$; **, $P < 0.01$.

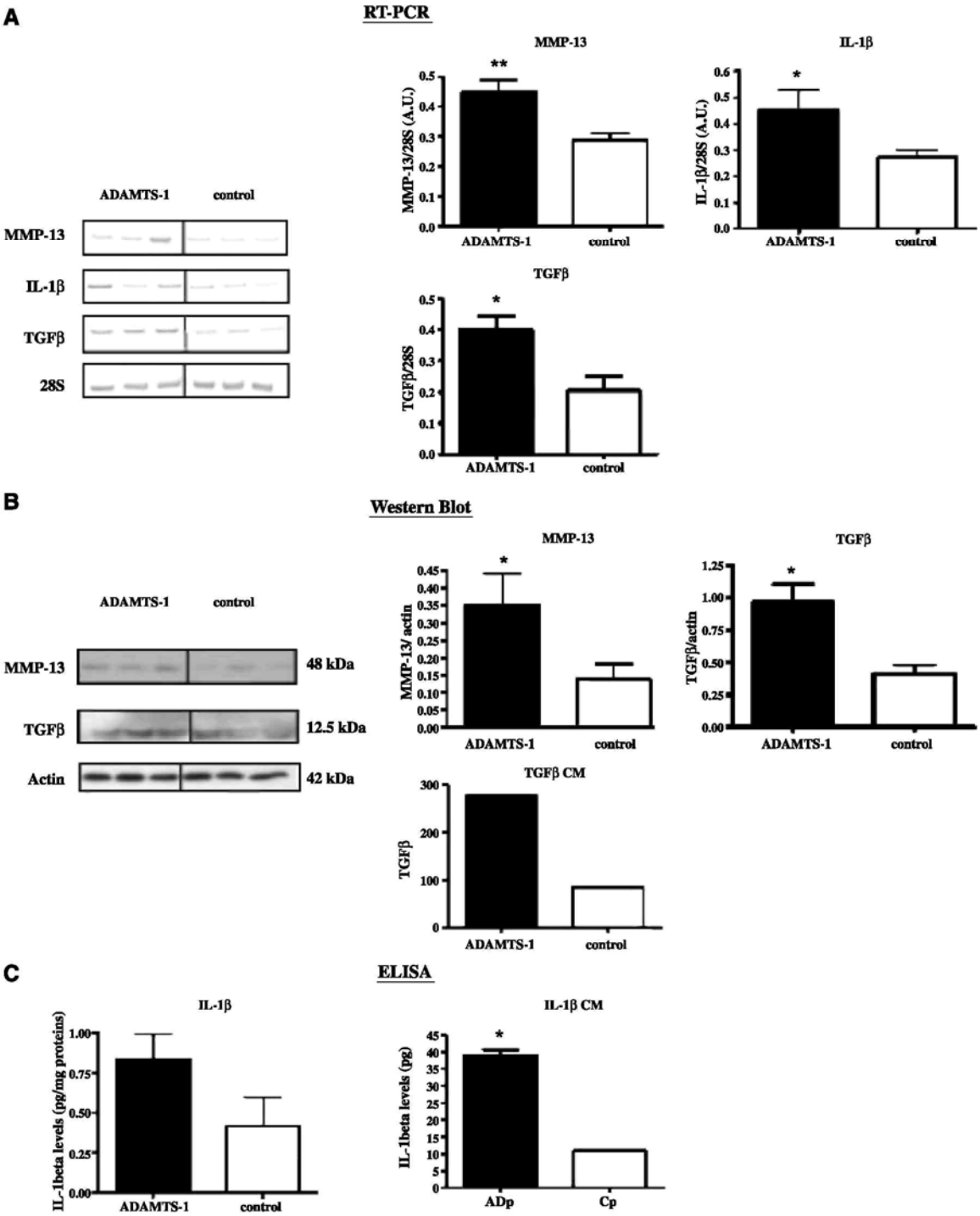

ADAMTS-1 promotes *in vitro* fibroblast chemoattraction.

To verify whether the catalytic activity of ADAMTS-1 is directly implicated in the recruitment of fibroblasts, we evaluated the ability of conditioned media from cell populations to attract fibroblasts in a 48-well chamber. The number of migrating fibroblasts was enhanced when the lower part of the chamber was filled with conditioned

media originating from ADAMTS-1-overexpressing populations ($P < 0.01$). Moreover, media conditioned by ADAMTS-1-overexpressing cells bearing an inactive catalytic site (ADp*) failed to enhance fibroblast migration. However, recombinant ADAMTS-1 added to medium conditioned by control cells is not per se sufficient to attract fibroblasts ($P < 0.01$; Fig. *6A)*. Interestingly, neutralizing anti-TGF-β and anti-IL-1β antibodies affected migration of fibroblast in a separate experiment ($P < 0.01$). It is worth noting that the inhibition of fibroblast migration was higher when anti-TGF-β and anti-IL-1β were both added to the medium conditioned by ADAMTS-1-overexpressing cells ($P < 0.005$; Fig. *6B)*. This suggests that these two factors induced by ADAMTS-1 expression contribute to induce fibroblast migration.

Figure 6: *ADAMTS-1 transfectants promote in vitro fibroblast chemoattraction.* A, fibroblasts were seeded on the upper compartment. The lower compartment was filled with 30 μL conditioned media of cell populations overexpressing (*ADp*) or not (*Cp*) ADAMTS-1. The importance of an intact catalytic domain was tested by using media conditioned by cells overexpressing a catalytically mutated form of ADAMTS-1 (*ADp**) or by their corresponding controls (*Cp2*). Recombinant ADAMTS-1 (*rADAMTS-1*, 5 μg/mL) was added (+) or not (-) to the lower compartment. Migration of fibroblasts was determined after 4 h of incubation by counting cell number on the lower face of the filter under a microscope at x400 magnification. **, $P < 0.01$. B, the assay was done as in A and anti-TGF-β and/ or anti-IL-1β neutralizing antibodies were added (+) or not (-) to the lower chamber. **, $P < 0.01$, versus Cp, ADp + anti-TGF-β, ADp + anti-IL-1 β, and ADp + anti-TGF-β + anti-IL-1 β.

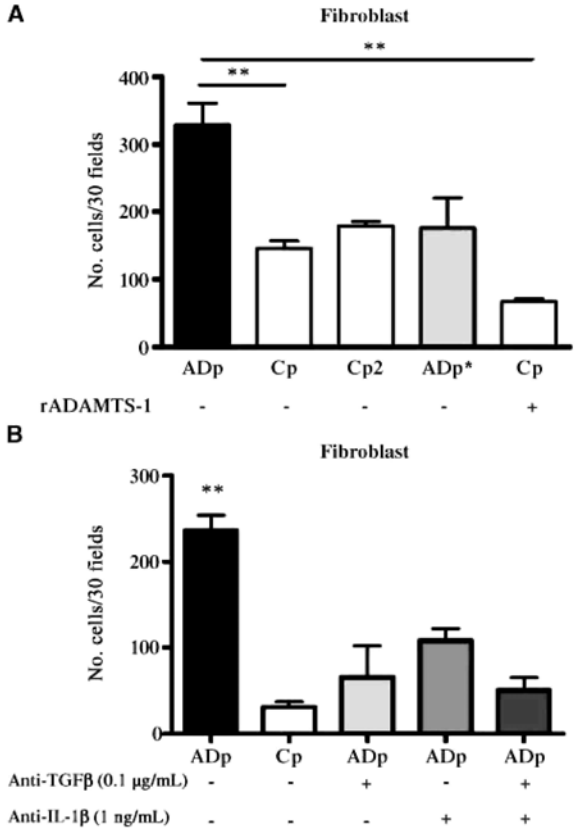

DISCUSSION

ADAMTS-1 is a multifunctional metalloproteinase whose expression has been detected in a variety of carcinomas (18, 20, 21, 31). Whether or not this enzyme promotes cancer development is currently a subject of controversy. In the present study, we have generated human bronchial BZR tumor cells overexpressing ADAMTS-1 or the proteinase-dead mutant of ADAMTS-1.

We report here that ADAMTS-1 overexpression accelerates tumor development and increases tumor cell proliferation rates after s.c. injection into SCID mice. This ADAMTS-1 tumor-promoting effect is associated with an enhanced stromal reaction evidenced by myofibroblasts infiltration and increased matrix deposition. Moreover, we show that the protumoral activity of ADAMTS-1 is dependent on the presence of an active metalloproteinase domain.

These data provide the first line of evidence for an implication of ADAMTS-1 in the stromal reaction associated to cancer development. Our study reveals the infiltration of tumors issued from ADAMTS-1-overexpressing cells by αSMA-positive cells corresponding to the recruitment of myofibroblasts, which have been described as key actors of tumor progression (2). To rule out the possibility that ADAMTS-1-overexpressing tumor cells could differentiate *in vivo* into mesenchymal-shaped cells, an *in situ* hybridization against the murine Y chromosome was assessed on tumor tissues and confirmed that host cells undergo a differentiation into myofibroblasts.

It is well established that tumor stroma influences cancer progression (3, 6, 7). Indeed, cancer-associated fibroblasts can directly influence tumor initiation and development either by secreting growth factors (2, 32-34) or by recruiting endothelial progenitor cells thereby promoting angiogenesis (35). In addition, cancer-associated fibroblasts are a source of extracellular matrix-degrading proteinases such as MMPs that are essential for both tumor progression and metastatic process. Indeed, fibroblasts deficient for MMP-11 (5) or MMP-14 (36, 37) lose their capacity to promote the implantation of tumor cells in nude mice. Moreover, MMP inhibition blocked the tumor-promoting effect of stromal cells (6). In this context, our data showing that ADAMTS-1 production promoted the recruitment of myofibroblasts in tumors suggest that ADAMTS-1 contributes to the elaboration of a reactive stroma permissive to tumor progression (3, 7).

In line with a previous study reporting that ADAMTS-1 stimulates fibroblast migration in a wound healing assay (38), we show here that ADAMTS-1-overproducing tumor cells promote fibroblast migration *in vitro.* This could not be attributed to a direct effect of ADAMTS-1 because the recombinant enzyme alone failed to modulate fibroblast migration. Instead, our data show that this effect on fibroblast chemotaxis could be ascribed to an increased production of TGF-β and IL-1β. This new concept is supported by two findings. First, higher amounts of these two mediators were detected at mRNA and protein levels both in tumors and in cells overexpressing ADAMTS-1. Second, anti-TGF-β and/or anti-IL-1β neutralizing antibodies blocked the chemo-tactic effect of medium conditioned by ADAMTS-1-producing cells on fibroblast migration. These results indicate that ADAMTS-1 production leads to an increased secretion of TGF-β and IL-1β, thereafter inducing the recruitment of fibroblasts and/or their differentiation into myofibroblasts. In addition, fibronectin, also exaggeratedly secreted by ADAMTS-1-overexpressing tumors, might also contribute to myofibroblast differentiation (39).

The collagen accumulation in tumors observed in this study may occur through different mechanisms including at least an overproduction of matrix components by fibroblasts and a remodeling of the matrix (25). Interstitial collagen matrix remodeling occurs through the action of interstitial collagenases including MMP-1, MMP-8, MMP-13, and, to some extent, MMP-14 (37,40-43). In our study, MMP-13 is the only interstitial collagenase displaying an increased expression in ADAMTS-1-overexpressing tumors and levels of MMP-13 expression are correlated to those of ADAMTS-1. MMP-13 is widely expressed in human malignant tumors (40, 44). In non-small-cell lung cancer, MMP-13 overproduction has recently been reported as a marker of poor prognosis (45). Moreover, in experimental models, targeted inhibition of MMP-13 inhibits tumor cell growth (46). MMP-13 could thus contribute to the enhanced tumor progression observed in the present study. When studied *in vitro,* ADAMTS-1 overexpres-sion did not affect gene expression and protein production of MMP-13 by tumor cells. A putative cellular source of MMP-13 in our model is the myofibroblasts recruited and activated by the tumor cells. This hypothesis is in line with a previous study showing that MMP-13 expression is increased in myofibroblasts from breast cancers (47). These findings further emphasize the importance of host-tumor interactions in tumor progression (7). Different hypotheses could explain the modulation of MMP-13 protein production *in vivo.* A first hypothesis is that higher numbers of myofibroblasts *in situ* result in higher production of MMP-13. Alternatively, specific modulations of cell signaling by ADAMTS-1 could interfere with MMP-13 expression. This is supported by our finding that there are higher phosphorylation levels for phosphatidylinositol 3-kinase in tumors issued from ADAMTS-1-overexpressing cells, whereas phosphorylation of p42/44, p38, or c-jun NH_2-terminal kinase is not affected[2].

Taken together, these data provide evidence for the contribution of ADAMTS-1 in tumor development and progression. Accordingly, a protumoral activity has been reported for the full-length molecule in Lewis lung carcinoma or TA3 mammary carcinoma models (24). It has been ascribed by the authors to an increased ADAMTS-1 proteolytic activity toward HB-EGF and amphiregulin (24). Nevertheless, in the present study, the ADAMTS-1-mediated effects do not rely on HB-EGF or amphiregulin cleavage (data not shown). In contrast, antitumor effects have been attributed to ADAMTS-1 fragments, which inhibit tumor cell proliferation and repress tumor angiogenesis (24). Furthermore, ADAMTS-1 inhibits endothelial cell proliferation *in vitro* and angiogenesis *in vivo* by sequestration of $VEGF_{165}$ (22, 48). In this study, however, we do not detect any

[2] Unpublished data

ADAMTS-1 fragments either *in vitro* or *in vivo*. In addition, no effect of ADAMTS-1 expression has been detected on the angiogenic response, both in tumors *in vivo* and in the aorta ring model *in vitro*. Therefore, the increased tumor development observed here is not linked to a modulation of angiogenesis. The effects observed in this work may rather rely on a paracrine effect resulting in enhanced production of factors recruiting fibroblasts, leading to the elaboration of a reactive stroma known to promote tumor development (3,4, 7). This novel mode of action identified in the present study does not exclude the possibility that ADAMTS-1 functions through multiple mechanisms. There is an apparent contradiction with the study published by Liu and colleagues showing that the increased expression of full-length molecule of ADAMTS-1 promotes angiogenesis. However, in this work, the effects of ADAMTS-1 overexpression on tumor invasion and angiogenesis require the shedding of the transmembrane precursors of HB-EGF and amphiregulin (24). In our work, however, the ADAMTS-1 overexpression is apparently not implicated in the cleavage of HB-EGF or amphiregulin but rather modulates other proteins implicated in different pathways, such as TGF-β and/or IL-1β. Moreover, some technical differences such as animal models and cell lines might also account for those discrepancies.

Our study provides new evidence for the large diversity of ADAMTS-1 functions in cancer. Overall, our work represents the first demonstration that a MMP-related enzyme contributes to the recruitment of myofibroblasts and collagen deposition in tumors concomitantly with an up-regulation of TGF-β and IL-1β. These data provide a new mechanism for ADAMTS-1 involvement in tumor development.

Disclosure of Potential Conflicts of Interest

No potential conflicts of interest were disclosed.

Acknowledgments

Grant support: Communauté française de Belgique (Actions de Recherches Concertées); the Fonds de la Recherche Scientifique Médicale; the Fonds National de la Recherche Scientifique (FNRS, Belgium); the Fonds spéciaux de la Recherche (University of Liège); the Fondation Léon Fredericq (University of Liège); the Direction générale des Technologies, de la Recherche et de l'Energie from the "Région Wallonne," the European Union Framework Programs (FP6 and FP7); and the Interuniversity Attraction Poles Program-Belgian Science Policy (Brussels, Belgium). N. Rocks is a fellow of the Télévie Program (FNRS, Belgium); D. Cataldo is a research associate from the FNRS; and G. Paulissen is a research fellow from the Fonds pour la Formation à la Recherche dans l'Industrie et dans l'Agriculture program (FNRS, Belgium).

The costs of publication of this article were defrayed in part by the payment of page charges. This article must therefore be hereby marked *advertisement* in accordance with 18 U.S.C. Section 1734 solely to indicate this fact.

We thank Christine Fink Fabrice Olivier, Fabienne Perin, Marie-Jeanne Nix, and Antoine Heyeres for their excellent technical assistance; Alain Colige and Betty Nusgens for helpful advice; and Silvia Blacher for quantification of aortic ring assay.

References

1. Hanahan D, Weinberg RA. The hallmarks of cancer. Cell 2000;100:57-70.

2. Kalluri R, Zeisberg M. Fibroblasts in cancer. Nat Rev Cancer 2006;6:392-401.

3. Mueller MM, Fusenig NE. Friends or foes—bipolar effects of the tumour stroma in cancer. Nat Rev Cancer 2004;4:839-49.

4. Tlsty TD, Hein PW. Know thy neighbor: stromal cells can contribute oncogenic signals. Curr Opin Genet Dev 2001;11:54-9.

5. Masson R, Lefebvre O, Noel A, et al. *In vivo* evidence that the stromelysin-3 metalloproteinase contributes in a paracrine manner to epithelial cell malignancy. J Cell Biol 1998;140:1535-41.

6. Noel A Hajitou A, L'Hoir C, et al. Inhibition of stromal matrix metalloproteases: effects on breast-tumor promotion by fibroblasts. Int J Cancer 1998;76:267-73.

7. Noel A, Jost M, Maquoi E. Matrix metalloproteinases at cancer tumor-host interface. Semin Cell Dev Biol 2008;19:52-60.

8. Liu D, Hornsby PJ. Senescent human fibroblasts increase the early growth of xenograft tumors via matrix metalloproteinase secretion. Cancer Res 2007; 67:3117-26.

9. Apte SS. A disintegrin-like and metalloprotease (reprolysin type) with thrombospondin type 1 motifs: the ADAMTS family. Int J Biochem Cell Biol 2004;36: 981-5.

10. Cal S, Obaya AJ, Llamazares M, Garabaya C, Quesada V, Lopez-Otin C. Cloning, expression analysis, and structural characterization of seven novel human ADAMTSs, a family of metalloproteinases with disinte-grin and thrombospondin-1 domains. Gene 2002;283: 49-62.

11. Mochizuki S, Okada Y. ADAMs in cancer cell proliferation and progression. Cancer Sci 2007;98:621-8.

12. Rocks N, Paulissen G, El Hour M, et al. Emerging roles of ADAM and ADAMTS metalloproteinases in cancer. Biochimie 2008;90:369-79.

13. Cauwe B, Van den Steen PE, Opdenakker G. The biochemical, biological, and pathological kaleidoscope of cell surface substrates processed by matrix metalloproteinases. Crit Rev Biochem Mol Biol 2007;42:113-85.

14. Colige A, Li SW, Sieron AL, Nusgens BV, Prockop DJ, Lapiere CM. cDNA cloning and expression of bovine procollagen I N-proteinase: a new member of the superfamily of zinc-metalloproteinases with binding sites for cells and other matrix components. Proc Natl Acad Sci U S A 1997;94:2374-9.

15. Kesteloot F, Desmouliere A, Leclercq I, et al. ADAM metallopeptidase with thrombospondin type 1 motif 2 inactivation reduces the extent and stability of carbon tetrachloride-induced hepatic fibrosis in mice. Hepatol-ogy 2007;46:1620-31.

16. Overall CM, Dean RA Degradomics: systems biology of the protease web. Pleiotropic roles of MMPs in cancer. Cancer Metastasis Rev 2006;25:69-75.

17. Llamazares M, Obaya AJ, Moncada-Pazos A, et al. The ADAMTS12 metalloproteinase exhibits anti-tumorigenic properties through modulation of the Ras-dependent ERK signalling pathway. J Cell Sci 2007;120:3544-52.

18. Porter S, Scott SD, Sassoon EM, et al. Dysregulated expression of adamalysin-thrombospondin genes in human breast carcinoma. Clin Cancer Res 2004;10: 2429-40.

19. Porter S, Span PN, Sweep FC, et al. ADAMTS8 and ADAMTS15 expression predicts survival in human breast carcinoma. Int J Cancer 2006;118:1241-7.

20. Rocks N, Paulissen G, Quesada CF, et al. Expression of a disintegrin and metalloprotease {ADAM and ADAMTS) enzymes in human non-small-cell lung carcinomas (NSCLC). Br J Cancer 2006;94:724-30.

21. Masui T, Hosotani R, Tsuji S, et al. Expression of METH-1 and METH-2 in pancreatic cancer. Clin Cancer Res 2001;7:3437-43.

22. Iruela-Arispe ML, Carpizo D, Luque A. ADAMTS1: a matrix metalloprotease with angioinhibitory properties. Ann N Y Acad Sci 2003;995:183-90.

23. Kuno K, Bannai K, Hakozaki M, Matsushima K, Hirose K. The carboxyl-terminal half region of ADAMTS-1 suppresses both tumorigenicity and experimental tumor metastatic potential. Biochem Biophys Res Commun 2004;319:1327-33.

24. Liu YJ, Xu Y, Yu Q. Full-length ADAMTS-1 and the ADAMTS-1 fragments display pro- and antimetastatic activity, respectively. Oncogene 2006;25:2452-67.

25. Noel A, Munaut C, Boulvain A, et al. Modulation of collagen and fibronectin synthesis in fibroblasts by normal and malignant cells. J Cell Biochem 1992;48: 150-61.

26. Laboisse CL, Augeron C, Potet F. Growth and differentiation of human gastrointestinal adenocarcinoma stem cells in soft agarose. Cancer Res 1981;41:310-5.

27. Blacher S, Devy L, Burbridge MF, et al. Improved quantification of angiogenesis in the rat aortic ring assay. Angiogenesis 2001;4:133-42.

28. Chabottaux V, Sounni NE, Pennington CJ, et al. Membrane-type 4 matrix metalloproteinase promotes breast cancer growth and metastases. Cancer Res 2006; 66:5165-72.

29. Noel A, Pauw-Gillet MC, Purnell G, Nusgens B, Lapiere CM, Foidart JM. Enhancement of tumorigenicity of human breast adenocarcinoma cells in nude mice by Matrigel and fibroblasts. Br J Cancer 1993;68: 909-15.

30. Bergman I, Loxley R. Two improved and simplified methods for determination of hydroxyproline. Anal Chem 1963;35:1961-5.

31. Kalinski T, Krueger S, Sel S, Werner K, Ropke M, Roessner A. ADAMTS 1 is regulated by interleukin-lβ, not by hypoxia, in chondrosarcoma. Hum Pathol 2007; 38:86-94.

32. Cat B, Stuhlmann D, Steinbrenner H, et al. Enhancement of tumor invasion depends on transdifferentiation of skin fibroblasts mediated by reactive oxygen species. J Cell Sci 2006;119:2727-38.

33. Kuperwasser C, Chavarria T, Wu M, et al. Reconstruction of functionally normal and malignant human breast tissues in mice. Proc Natl Acad Sci USA 2004; 101:4966-71.

34. Olumi AF, Grossfeld GD, Hayward SW, Carroll PR, Tlsty TD, Cunha GR. Carcinoma-associated fibroblasts direct tumor progression of initiated human prostatic epithelium. Cancer Res 1999;59:5002-11.

35. Orimo A, Gupta PB, Sgroi DC, et al. Stromal fibroblasts present in invasive human breast carcinomas promote tumor growth and angiogenesis through elevated SDF-1/CXCL12 secretion. Cell 2005;121:335-48.

36. Zhang W, Matrisian LM, Holmbeck K, Vick CC, Rosenthal EL. Fibroblast-derived MT1-MMP promotes tumor progression *in vitro* and *in vivo.* BMC Cancer 2006;6:52.

37. Szabova L, Chrysovergis K, Yamada SS, Holmbeck K. MTl-MMP is required for efficient tumor dissemination in experimental metastatic disease. Oncogene 2008;27: 3274-81.

38. Krampert M, Kuenzle S, Thai SN, Lee N, Iruela-Arispe ML, Werner S. ADAMTSl proteinase is up-regulated in wounded skin and regulates migration of fibroblasts and endothelial cells. J Biol Chem 2005;280:23844-52.

39. Desmouliere A. Factors influencing myofibroblast differentiation during wound healing and fibrosis. Cell Biol Int 1995;19:471-6.

40. Ala-Aho R, Kahari VM. Collagenases in cancer. Biochimie 2005;87:273-86.

41. Benbow U, Schoenermark MP, Mitchell TI, et al. A novel host/tumor cell interaction activates matrix metalloproteinase 1 and mediates invasion through type I collagen. J Biol Chem 1999;274:25371-8.

42. Pendas AM, Uria JA, Jimenez MG, Balbin M, Freije JP, Lopez-Otin C. An overview of collagenase-3 expression in malignant tumors and analysis of its potential value as a target in antitumor therapies. Clin Chim Acta 2000; 291:137-55.

43. Freije JM, Diez-Itza I, Balbin M, et al. Molecular cloning and expression of collagenase-3, a novel human matrix metalloproteinase produced by breast carcinomas. J Biol Chem 1994;269:16766-73.

44. Balbin M, Pendas AM, Uria JA, Jimenez MG, Freije JP, Lopez-Otin C. Expression and regulation of collagenase-3 (MMP-13) in human malignant tumors. APMIS 1999; 107:45-53.

45. Hsu CP, Shen GH, Ko JL. Matrix metalloproteinase-13 expression is associated with bone marrow micro-involvement and prognosis in non-small cell lung cancer. Lung Cancer 2006;52:349-57.

46. Ala-aho R, Ahonen M, George SJ, et al. Targeted inhibition of human collagenase-3 (MMP-13) expression inhibits squamous cell carcinoma growth *in vivo.* Oncogene 2004;23:5111-23.

47. Nielsen BS, Rank F, Lopez JM, et al. Collagenase-3 expression in breast myofibroblasts as a molecular marker of transition of ductal carcinoma *in situ* lesions to invasive ductal carcinomas. Cancer Res 2001;61:7091-100.

48. Luque A, Carpizo DR, Iruela-Arispe ML. ADAMTS1/ METH1 inhibits endothelial cell proliferation by direct binding and sequestration of VEGF165. J Biol Chem 2003;278:23656-65.